

Article

Preparation of Polyphenylene Ring Derivative Dyes with Wide Wave Absorption Properties and Their Performance Study

Yuzhen Zhao ^{1,†}, Xinhua Liu ^{2,†}, Qing Li ¹, Zhun Guo ¹, Zemin He ¹, Huimin Zhang ¹, Cheng Ma ¹, Jianjing Gao ¹, Yang Zhao ² and Dong Wang ^{2,*}

¹ Xi'an Key Laboratory of Advanced Photo-Electronics Materials and Energy Conversion Device, School of Electronic Information, Xijing University, Xi'an 710123, China

² Department of Materials Physics and Chemistry, School of Materials Science and Engineering, University of Science and Technology Beijing, Beijing 100083, China

* Correspondence: wangdong@ustb.edu.cn

† These authors contributed equally to this work.

Abstract: Some conjugated benzene ring molecules were prepared using the Sonogashira reaction, and the molecules were post-functionally modified using click chemistry. The optical and electrical band gaps were measured using UV-VIS absorption spectroscopy and the three-electrode method, and the results of both were verified against each other to prove the accuracy of the characterization. In addition, the optical performances of the material were studied by z-scan; almost all materials exhibited good nonlinear optical properties and interconversion between saturable and anti-saturable absorption due to the invocation of click reagents.

Keywords: Azobenzene; click chemistry; nonlinear optics



Citation: Zhao, Y.; Liu, X.; Li, Q.; Guo, Z.; He, Z.; Zhang, H.; Ma, C.; Gao, J.; Zhao, Y.; Wang, D.

Preparation of Polyphenylene Ring Derivative Dyes with Wide Wave Absorption Properties and Their Performance Study. *Molecules* **2022**, *27*, 5551. <https://doi.org/10.3390/molecules27175551>

Academic Editor: Eric Defrancq

Received: 4 August 2022

Accepted: 24 August 2022

Published: 29 August 2022

Publisher's Note: MDPI stays neutral with regard to jurisdictional claims in published maps and institutional affiliations.



Copyright: © 2022 by the authors. Licensee MDPI, Basel, Switzerland. This article is an open access article distributed under the terms and conditions of the Creative Commons Attribution (CC BY) license (<https://creativecommons.org/licenses/by/4.0/>).

1. Introduction

In recent years, many small molecules with excellent nonlinear optical properties have entered the limelight because of promising potential in a wide diversity of optical fields, for example, quantum communication, optical limiting, and information storage [1–3]. Organic small molecules have excellent properties such as diverse structural composition and wide space for property tuning, and the molecules can be designed to tune the actually desired properties. However, the preparation of current small-molecule conjugated materials is very complicated, and the chemical synthesis and purification are very tedious, which limits its development in some cases [4–7].

The emergence of click chemistry has effectively solved this problem. The click chemistry occurs in fast, side-reaction-free, near-100% yields and is easily purified [8,9]. The introduction of click chemistry into the preparation of nonlinear materials has led to the synthesis of a wide variety of organic small molecule nonlinear materials that express strong nonlinearity [10–13].

Traditionally, biphenyl-like molecules are widely used in pharmaceuticals, pesticides, dyes, liquid crystal materials [14–17], and also in the manufacture of fuels, engineering plastics, and high-energy fuels [18–20]. However, Biphenyl materials are rarely used as non-linear optical materials.

In this paper, a biphenyl-based conjugated structure molecule was constructed by Sonogashira coupling reaction and functionalized by click reagents, and the effects of different amounts and categories of click reagents on the molecular properties were investigated. The results indicate that these functionally modified molecules show a wide absorption. The type of click reagent has a strong influence on the molecular properties, compared to the symmetry of the molecule and the number of click reagents, which have less influence.

2. Preparation and Research

2.1. Preparation

The synthetic route of dibiphenyl derivatives is placed in Figure 1. Monobromobiphenyl and dibromobiphenyl and N, N-dibutyl-4-ethynylaniline are firstly used as raw materials and the target dibiphenyl derivatives are obtained in moderate yields by linking the two by Sonogashira coupling reaction. The dibiphenyl derivatives have two clickable triple bonds, to which different electron acceptors are introduced by a two-step click reaction, resulting in five molecules with different click structures. The yields of the different structural click products are presented in detail in the experimental section. Due to the difference in the number and structure of the introduced acceptor molecules, the polarity of all the obtained click products varies widely, which makes the separation of the click products very simple.

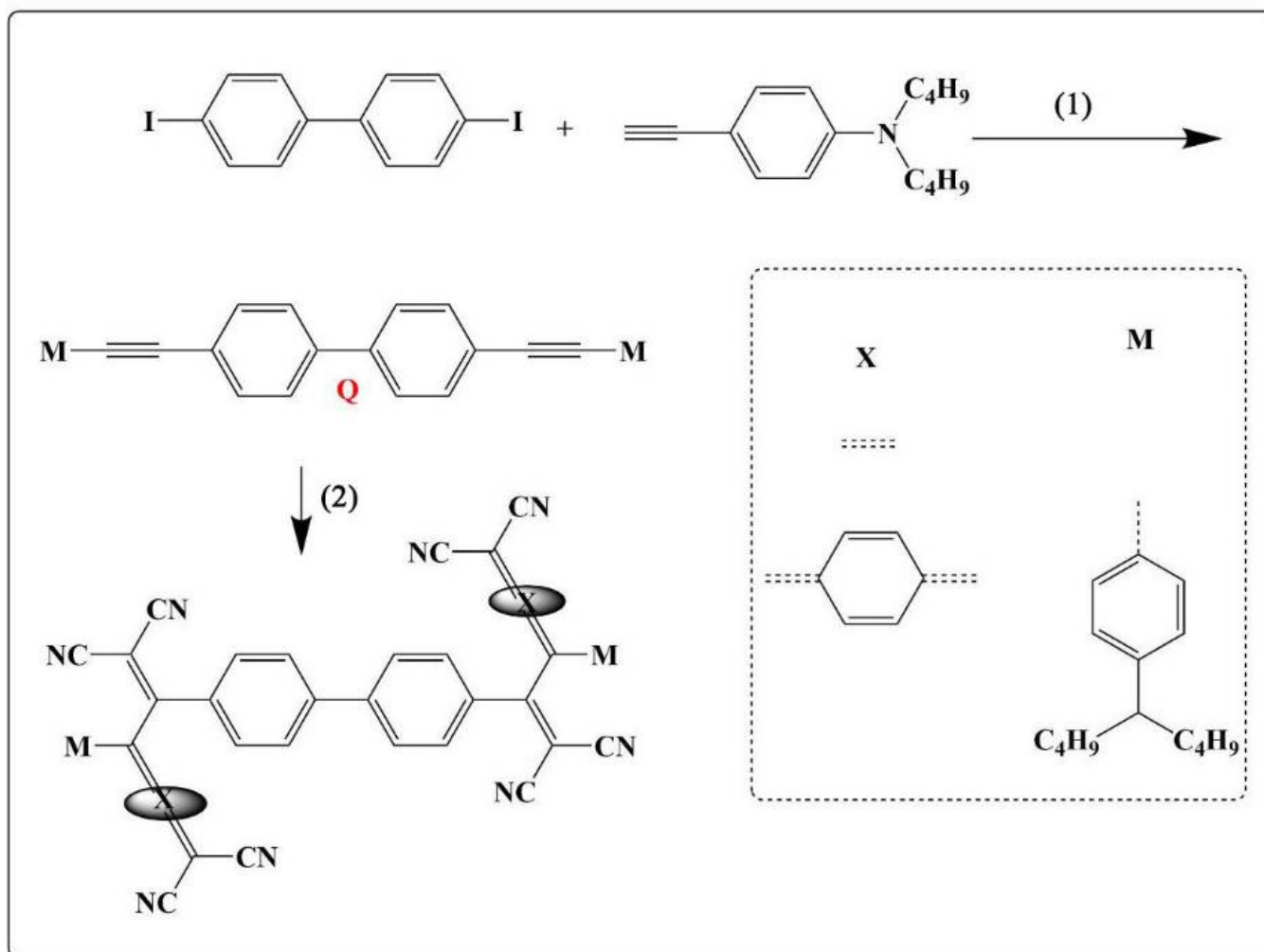


Figure 1. Cont.

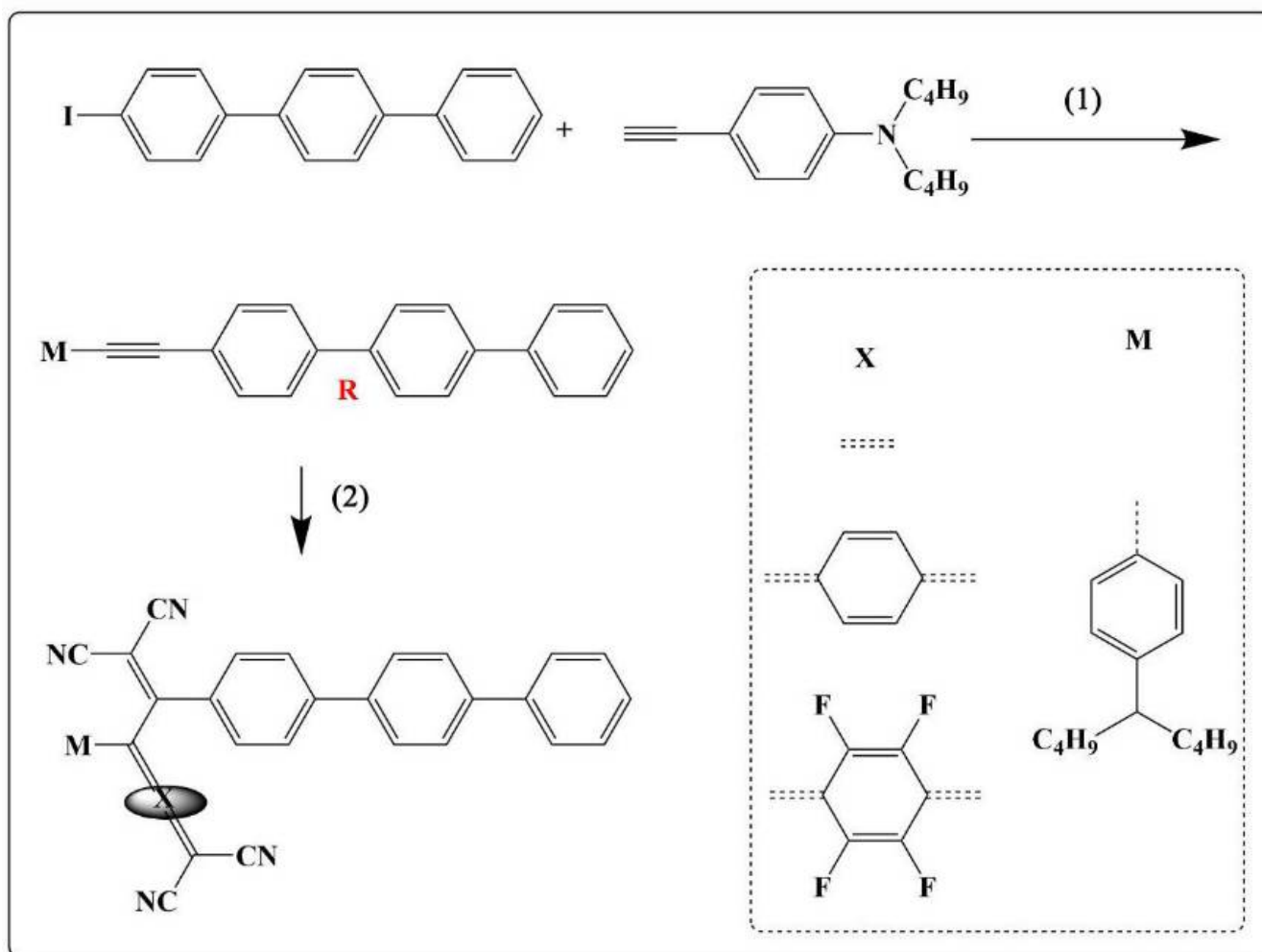


Figure 1. Total Synthesis route (1) $\text{PdCl}_2(\text{PPh}_3)$, CuI , DIPA, 60°C , Ar, 36 h; (2) TCNE/TCNQ/F4-TCNQ, CH_2Cl_2 , rt, 1 h.

2.2. UV-Vis-NIR Spectro

To study the occurrence of click chemistry and its occurrence or not of side reactions, a click-track reaction is carried out in this paper using compound Q. The TCNE is titrated to Q in a fixed amount twenty times, and the progress of the reaction is monitored by UV-Vis spectroscopy. The titration experiments of 0–1 equivalents of TCNE are shown in Figure 2a. When 0.1 equivalents of TCNE are added to the CH_2Cl_2 solution, the absorption peak of the precursor (Q) at 376 nm started to decrease, and an absorption peak occurred in 470 nm, which represents the production of new compounds (Q-1, Q-11). As TCNE is continuously added to the solution, the absorption peak at 470 nm gradually increased until the absorption peak at 376 nm decreased to a minimum after the addition of 2 equivalents of TCNE, which indicates the complete conversion of Q to Q-11. In previous works [21–26], click chemistry is shown to be efficient and free of side reactions. In Figure 2a, the production of extinction dots at 348 nm and 405 nm proves that the click reaction is side-reaction free.

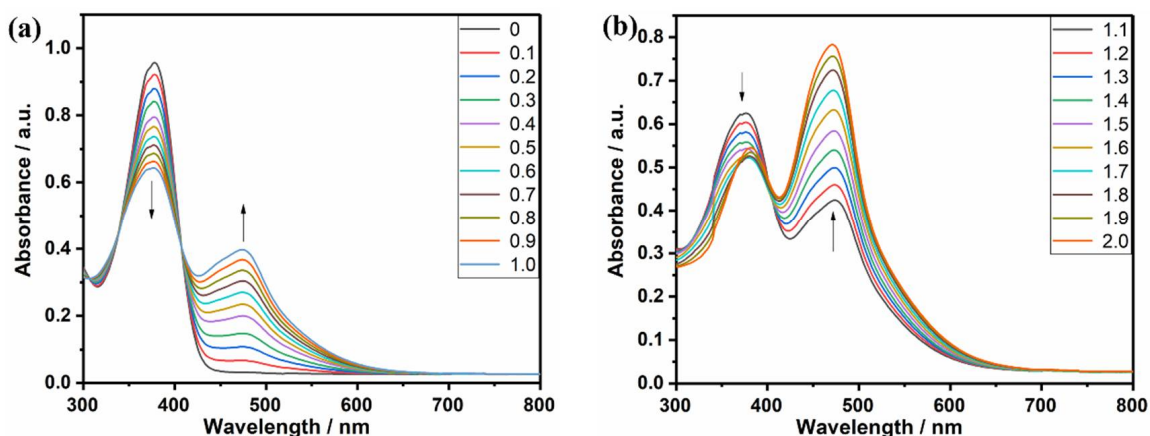


Figure 2. UV-VIS-NIR tracking spectrum of click response (a) TCNE (0–1.0 equivalent); (b) TCNE (1.0–2.0 equivalent).

Figure 3 shows the CH_2Cl_2 solution of the click-modified products of R and Q. Figure 4a shows the UV-VIS-NIR spectroscopy of the compounds in the CH_2Cl_2 solution. The reaction of the light-yellow molecule R with one equivalent of the click reagents TCNE, TCNQ, and F4-TCNQ give brown R-1, green R-2, and purple R-3, respectively. In Figure 4b, the same redshift occurs in the click product of Q.



Figure 3. CH_2Cl_2 solution of click modification products of R and Q.

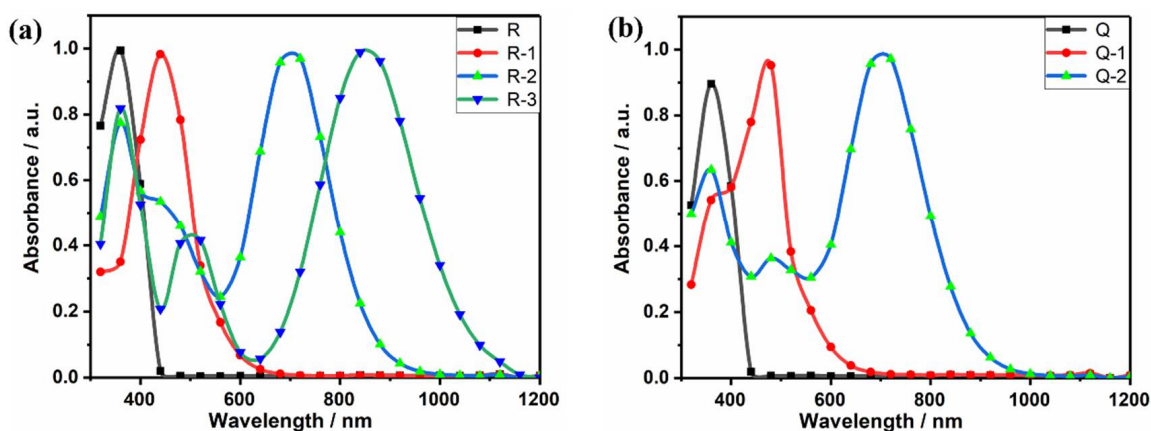


Figure 4. Absorption spectra of (a) R, R-1, R-2, R-3; (b) Q, Q-1, Q-2 in CH_2Cl_2 solution.

The main reason for the occurrence of the red-shift phenomenon is the introduction of click reagents that grow the conjugate length of the backbone and enhance the electron affinity [27,28]. The absorption peak of R-3 shows a larger redshift than R-1 and R-2, which

is due to the introduction of strong electron-absorbing groups-CN and -F, which have a more pronounced effect of extending the conjugation length of the molecule. Compared with R, Q has two clickable triple bonds, so two acceptor molecules can be introduced. However, in Figure 4b, Q-11, Q-22 with two acceptor molecules introduced to show the same redshift of the maximum absorption peaks relative to R-1, R-2 with one acceptor molecule introduced, and the absorption peaks do not shift due to the different number of clickable reagents introduced, which indicates that the symmetry of the molecule has almost no effect on the position of the maximum absorption peak, and the type of click reagent has the greatest effect on redshift.

In conclusion, the introduction of click reagents can prolong the conjugation length of molecules, thus causing movement of the maximum peak, the degree of movement varies depending on the type of click reagents, resulting in a series of broadband absorbing dyes that can absorb different wavelengths.

2.3. Electrochemistry

Electron off-domain is related to the nonlinear nature [25,29,30]. Figure 5 shows the cycle voltammogram and Figure 6 shows the energy level results of the compound. Table 1 also shows the initial redox potential. Electrical and optical energy bandwidths can be well matched, and both tend to decrease, thanks to the introduction of the acceptor molecules [31,32].

Table 1. Electrical properties of molecules.

Molecules	λ_{end}^a (nm)	E_g^b (eV)	$E_{on}^{ox}^c$ (V)	$E_{on}^{red}^c$ (V)	HOMO (eV)	LUMO (eV)	E_g^d (eV)
R	412	3.00	1.25	−1.08	−5.85	−3.52	2.33
R-1	692	1.79	0.88	−0.83	−5.48	−3.77	1.71
R-2	982	1.26	0.62	−0.61	−5.22	−3.99	1.23
R-3	1188	1.04	0.50	−0.42	−5.10	−4.18	0.92
Q	442	2.80	1.15	−1.02	−5.75	−3.58	2.17
Q-11	686	1.80	0.86	−0.80	−5.46	−3.80	1.66
Q-22	1006	1.23	0.61	−0.59	−5.21	−4.01	1.20

^a UV-VIS spectrum cut-off absorption wavelength. ^b Optical energy bandwidth. ^c Initial oxidation potential and initial reduction potential (obtained by cyclic voltammetry characteristic curve). ^d Electrochemical band gaps.

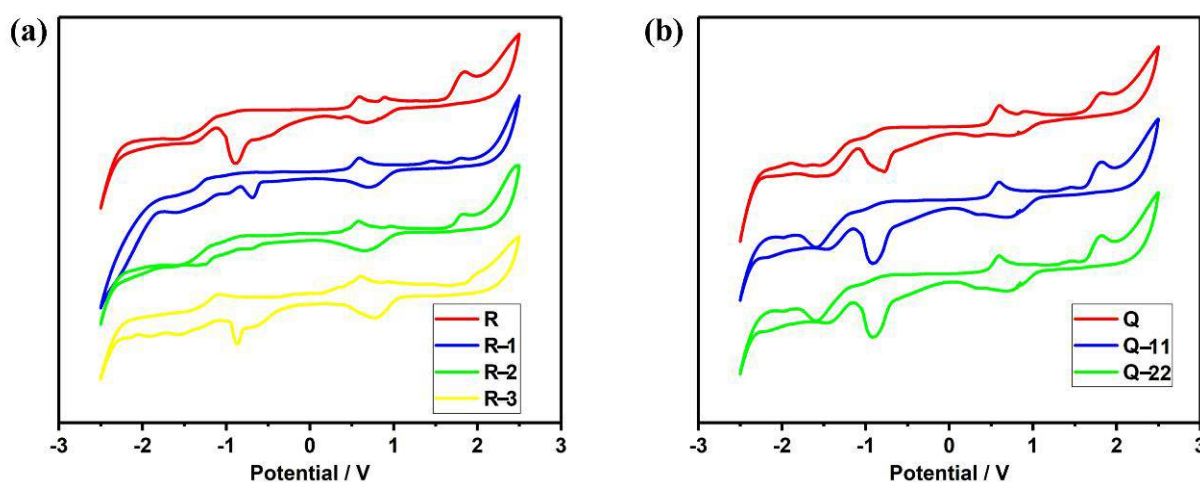


Figure 5. Cycle voltammogram of the molecular (a) R, R-1, R-2, R-3; (b) Q, Q-11, Q-22 in $\text{CH}_2\text{Cl}_2/\text{Bu}_4\text{NPF}_6$ at 298 K.

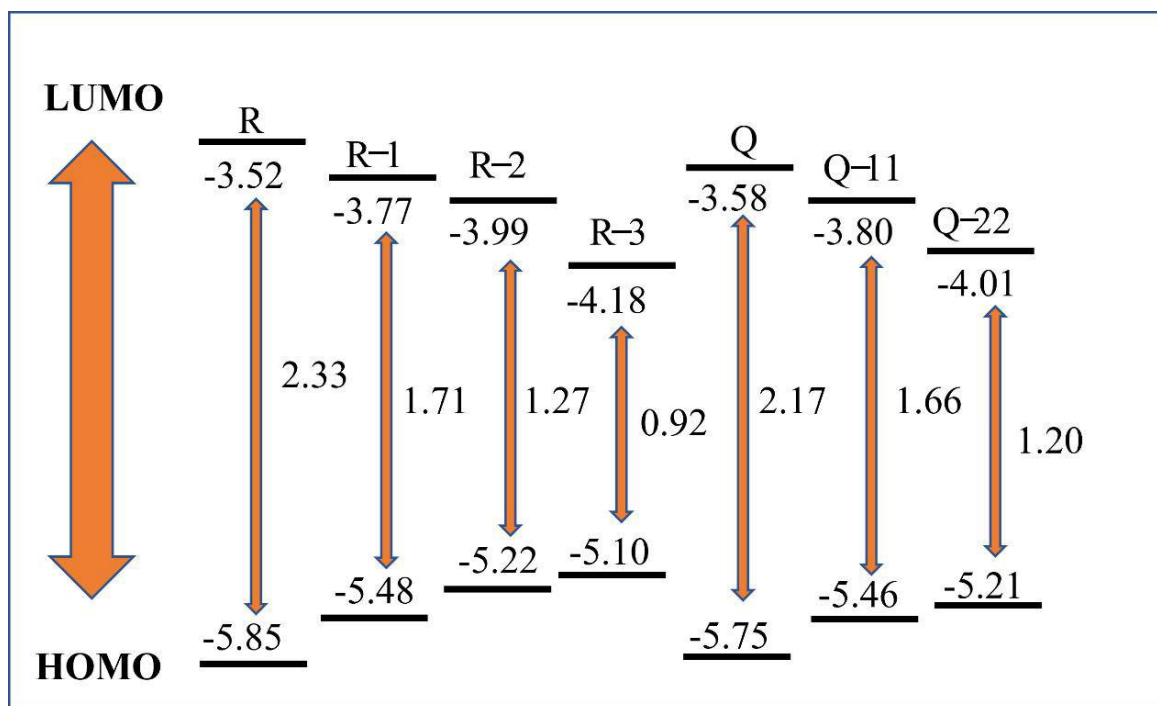


Figure 6. Electrical energy bands of benzene ring derivatives.

After the introduction of click reagents, the LUMO levels and band gaps of R-1, R-2, and R-3 showed a decreasing trend and the HOMO levels increased, and the band gap of R-3 decreased most significantly compared with R-1 and R-2, because of the groups -F and -CN in F4-TCNQ. Similarly, Q, Q-11, Q-22 show the same effect. By comparing R-1 and Q-11, R-2 and Q-22, it can be seen that the introduction of more click reagents in the molecule is less effective in reducing the bandgap, which can also indicate that the degree of conjugation of the molecule has a greater effect on the electrochemistry than the symmetry of the molecule. This is because the symmetry of the molecule has little effect on the degree of conjugation and does not change the conjugation structure, while the different kinds of click reagents introduced lengthen the conjugation length of the molecule, reduce the electron cloud density and the energy of the system, accelerate the intramolecular charge transfer, narrow the molecular band gap and make it easier for the leap.

2.4. Nonlinear Optics

The third-order nonlinear polarizability is one of the important parameters of the material [33]. The materials in this paper are tested under picosecond laser, some of them have poor nonlinear refractive properties, therefore, only the nonlinear absorption properties of the materials are investigated in this paper.

The Z-scan results of molecules are placed in Figure 7. No nonlinear optical properties are observed for molecule R which are shown in Table 2. Therefore, only R-1, R-2, R-3 are compared. It can be seen that after the click reaction, R-1 and R-3 have a peak in transmittance at the focal point and exhibit saturable absorption properties (SA), while R-2 has a valley in transmittance at the focal point and exhibits anti-saturation absorption properties (RSA), due to the alteration of the length of the molecular conjugate group as a result of the introduction of the click reagent, leading to a saturable absorption-trans-saturable absorption transition. The factors affecting the saturable to anti-saturable absorption transition are the absorption cross-section and the horizontal lifetime [34].

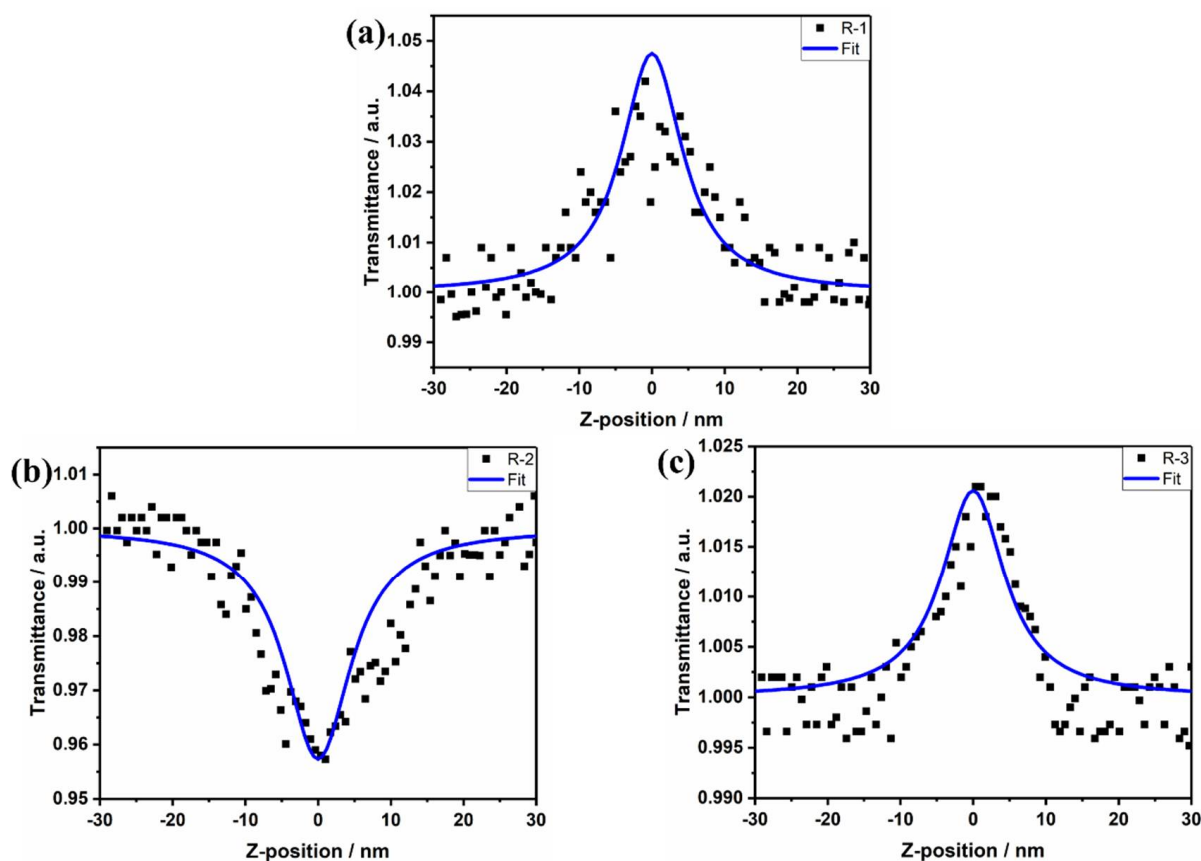


Figure 7. (a) R-1, (b) R-2, (c) R-3 Z-scan curves. The red line is the fitted data, and the scattered points are the Z-scan experimental data.

Table 2. Nonlinear data for molecules.

Molecules	$\beta \times 10^{-17}$ (m/W)	$\chi^{(3)} \times 10^{-17}$ (esu)
R-1	−30	6.45
R-2	30	6.45
R-3	−20	4.30
Q	15	3.23
Q-11	−33	7.09
Q-22	13	2.79

3. Materials and Methods

3.1. Material and Instrumental Characterization Equipment

All reagents were purchased from company sources and were ready for use. ^1H NMR spectra of the materials were measured using a BRUKER AVANCEIIIHD400 with deuterated chloroform as the solvent and tetramethylsilane (TMS) as the internal standard. The UV absorption was measured by a JASCO V-570 spectrophotometer. The instruments for mass spectrometry analysis of materials were AB SCIEX MALDI-TOF/TOF 5800. Cyclic voltammetric curves of materials were measured using the CHI 660C instrument. Measurement of the response of nonlinear optical (NLO) characteristics uses a Z-scan technique (NLO-Z), where the laser pulse is chosen to be 21 ps.

3.2. Preparation of Materials

3.2.1. Preparation of the Molecular R

N,N-dibutyl-4-ethynylaniline obtained from previous work [35] (1.6488 g, 0.0072 mol), 4-iodobiphenyl (0.6722 mg, 0.0024 mol), $[\text{PdCh}(\text{PPh}_3)]$ (0.00017 mol, 0.1206 g), CuI (0.00017 mmol, 0.034 g) were placed in the flask and 30 mL *i*PrNH was added, then shaken

for 36 h at 60 °C. After the temperature dropped to room temperature, the solvent was cleared, and the separation technology column chromatography, the eluent is CH₂Cl₂, and the first crude purification was performed to remove the catalyst in the system. Then the product was purified by column chromatography and after distillation under reduced pressure, 566 mg of light-yellow solid product R was obtained, with a yield of 62%.

¹H NMR (400 MHz, CDCl₃, δ): 7.66–7.60 (m, 4H), 7.58 (s, 8H), 7.50–7.44 (m, 4H), 7.43–7.35 (m, 6H), 6.64–6.59 (m, 4H), 3.37–3.26 (m, 8H), 1.66–1.58 (m, 8H), 1.41 (m, 8H), 0.99 (m, 12H). IR (neat): 2964, 2937, 2873, 2202, 1590, 1526, 1376, 1200, 814, 773, 692, 542. MALDI-TOF-MS (dithranol): *m/z*: [MH]⁺ calcd. for C₂₈H₃₁N: 381.25, found: 382.76. Elemental analysis calcd. (%) for C₂₈H₃₁N (381.25): C 88.14, N 3.67, H 8.19, found: C 88.12, N 3.66, H 8.22.

3.2.2. Preparation of the Molecular R-1

Compound R (152.4 mg, 0.4 mmol) was dissolved in 30 mL CH₂Cl₂ and TCNE (0.0512 g, 0.0004 mol) was added to it, then stirred for 40 min. After the reaction is over, the solvent was removed by distillation under reduced pressure, then a chromatographic column (the eluent is CH₂Cl₂) was used for purification to give R-1 (199.6 mg, 98%).

¹H NMR (400 MHz, CDCl₃, δ): 7.90–7.81 (m, 8H), 7.8–7.75 (m, 4H), 7.67–7.61 (m, 4H), 7.55–7.43 (m, 6H), 6.75–6.69 (m, 4H), 3.49–3.38 (m, 8H), 1.73–1.61 (m, 8H), 1.41 (m, 8H), 1.01 (m, 12H). IR (neat): 2959, 2869, 2220, 1603, 1490, 1340, 1209, 1181, 810, 769, 683, 578. MALDI-TOF-MS (dithranol): *m/z*: [M] calcd. For C₃₄H₃₁N₅: 509.26, found: 509.69. Elemental analysis calcd. (%) for C₃₄H₃₁N₅ (509.26): C 80.13, H 6.13, N 13.74, found: C 80.10, H 6.16, N 13.74.

3.2.3. Preparation of the Molecular R-2

Compound R (152.4 mg, 0.4 mmol) was dissolved in 30 mL CH₂Cl₂ and TCNQ (0.0817 g, 0.0004 mol) was added to it, then stirred for 40 min. After the reaction is over, the solvent was removed by distillation under reduced pressure. Then a chromatographic column was used for purification to give R-2 (226.98 mg, 97%).

¹H NMR (400 MHz, CDCl₃, δ): 7.83–7.78 (m, 4H), 7.75–7.70 (m, 4H), 7.65–7.55 (m, 6H), 7.53–7.42 (m, 6H), 7.31 (m, 6H), 7.09 (m, 4H), 6.75–6.69 (m, 4H), 3.46–3.37 (m, 8H), 1.69–1.61 (m, 8H), 1.46–1.37 (m, 8H), 1.01 (m, 12H). IR (neat): 2969, 2933, 2869, 2197, 1586, 1399, 1345, 1177, 932, 833, 764, 733, 687, 542. MALDI-TOF-MS (dithranol): *m/z*: [M] calcd. for C₄₀H₃₅N₅: 585.29, found: 585.96. Elemental analysis calcd. (%) for C₄₀H₃₅N₅ (585.29): C 82.02, N 11.96, H 6.02, found: C 82.00, N 11.95, H 6.05.

3.2.4. Preparation of the Molecular R-3

Compound R (152.4 mg, 0.4 mmol) was dissolved in 30 mL CH₂Cl₂ and F4-TCNQ (0.112 g, 0.0004 mol) was added to it, then stirred for 40 min. After the reaction is over, the CH₂Cl₂ was cleared by distillation, and then a chromatographic column was used for purification to give R-3 (259.1 mg, 98%), as a black solid.

¹H NMR (400 MHz, CDCl₃, δ): 7.77–7.72 (m, 4H), 7.72–7.67 (m, 4H), 7.66–7.61 (m, 4H), 7.54–7.44 (m, 6H), 7.40 (m, 4H), 6.89–6.84 (m, 4H), 3.59 (m, 8H), 1.76 (m, 8H), 1.50 (m, 8H), 1.05 (m, 12H). IR (neat): 2959, 2924, 2873, 2194, 1608, 1390, 1191, 1028, 964, 810, 778, 638, 533. MALDI-TOF-MS (dithranol): *m/z*: [M] calcd. for C₅₇H₅₅F₃N₈: 657.25, found: 657.77. Elemental analysis calcd. (%) for C₄₀H₃₁F₄N₅ (657.25): C 73.05, N 10.65, H 4.75, F 11.55, found: C 73.03, N 10.64, H 4.78, F 11.55.

3.2.5. Preparation of the Molecular Q

N,N-dibutyl-4-ethynylaniline obtained from previous work [34] (1648.8 mg, 7.2 mmol), 4,4'-diiodobiphenyl (974.4 mg, 2.4 mmol), [PdCh (PPh₃)] (120.6 mg, 0.172 mmol), CuI (34.0 mg, 0.178 mmol) were placed in the flask and 30 mL iPrNH was added, shaken for 36 h at 60 °C. After the temperature dropped to room temperature, the solvent was cleared, and the separation technology column chromatography, the eluent was CH₂Cl₂, and the

first crude purification was performed to remove the catalyst in the system. Then the product was refined and after distillation under reduced pressure, 846.3 mg of light-yellow solid product Q was obtained, with a yield of 58%.

^1H NMR (400 MHz, CDCl_3 , δ): 7.59 (d, $J = 1.6$ Hz, 4H), 7.46–7.33 (m, 2H), 6.66–6.55 (m, 2H), 3.37–3.27 (m, 4H), 1.59 (m, 4H), 1.39 (m, 4H), 0.99 (m, 6H). IR (neat): 2955, 2924, 2856, 2212, 1599, 1526, 1363, 1295, 1191, 1100, 1000, 928, 805, 533. MALDI-TOF-MS (dithranol): m/z : $[\text{MH}]^+$ calcd. for $\text{C}_{44}\text{H}_{52}\text{N}_2$: 608.41, found: 609.87. Elemental analysis calcd. (%) for $\text{C}_{44}\text{H}_{52}\text{N}_2$ (608.41): C 86.79, N 4.60, H 8.61, found: C 86.77, N 4.60, H 8.63.

3.2.6. Preparation of the Molecular Q-11

Molecular Q (0.243 g, 0.0004 mol) was dissolved in CH_2Cl_2 and TCNE (0.102 g, 0.0008 mol) was added, then stirred for 40 min. After the reaction was over, the solvent was removed by distillation under reduced pressure, and then a chromatographic column was used for purification to give Q-11 (331.7 mg, 96%).

^1H NMR (400 MHz, CDCl_3 , δ): 7.91–7.76 (m, 6H), 6.76–6.70 (m, 2H), 3.49–3.39 (m, 4H), 1.72–1.60 (m, 4H), 1.42 (m, 4H), 1.01 (m, 6H). IR (neat): 2969, 2938, 2873, 2206, 1603, 1485, 1422, 1345, 1191, 1000, 919, 814, 741, 545. MALDI-TOF-MS (dithranol): m/z : $[\text{M}]$ calcd. for $\text{C}_{56}\text{H}_{52}\text{N}_{10}$: 864.44, found: 864.84. Elemental analysis calcd. (%) for $\text{C}_{56}\text{H}_{52}\text{N}_{10}$ (864.44): C 77.75, N 16.19, H 6.06, found: C 77.73, N 16.18, H 6.09.

3.2.7. Preparation of the Molecular Q-22

Compound Q (0.243 g, 0.0004 mol) was dissolved in CH_2Cl_2 and TCNQ (0.166 g, 0.0008 mol) was added to it, then stirred for 40 min. After the reaction was over, the CH_2Cl_2 was cleared by distillation, then a chromatographic column for purification was used to give Q-22 (389.1 mg, 95%).

^1H NMR (400 MHz, CDCl_3 , δ): 8.14–7.75 (m, 4H), 7.75–7.49 (m, 4H), 7.05 (m, 2H), 6.71 (d, $J = 9.2$ Hz, 2H), 3.40 (m, 4H), 1.42 (m, 4H), 1.21 (m, 4H), 1.01 (m, 6H). IR (neat): 2964, 2918, 2873, 2202, 1571, 1404, 1340, 1187, 914, 846, 678, 532. MALDI-TOF-MS (dithranol): m/z : $[\text{MH}]^+$ calcd. for $\text{C}_{68}\text{H}_{60}\text{N}_{10}$: 1016.50, found: 1017.88. Elemental analysis calcd. (%) for $\text{C}_{68}\text{H}_{60}\text{N}_{10}$ (1016.50): C 80.29, N 13.77, H 5.95, found: C 80.27, N 13.77, H 5.97.

4. Conclusions

Some benzene ring derivatives were prepared and systematically studied. UV-VIS-NIR spectroscopy and electrical testing showed that the introduction of click reagents increased the conjugate groups of the molecules, caused a movement of the maximum peak, while the energy bandwidth of the click products was reduced to different degrees. Z-scan tests showed that after clicking, the molecules all showed different nonlinear properties, and with the use of different click reagents, the molecules could undergo a transition between anti-saturation absorption and saturation absorption, yielding nonlinear materials with different properties.

Author Contributions: Conceptualization, Y.Z. (Yuzhen Zhao) and X.L.; methodology, Q.L.; investigation, Y.Z. (Yuzhen Zhao), Z.G. and C.M.; data curation, Z.H. and H.Z.; writing—original draft preparation, Y.Z. (Yuzhen Zhao) and Y.Z. (Yang Zhao); writing—review and editing, D.W. and J.G.; supervision, D.W.; funding acquisition, D.W. All authors have read and agreed to the published version of the manuscript.

Funding: This work was supported by the National Natural Science Foundation of China (Grant No. 52173263), Natural Science Basic Research Program of Shaanxi (Program No. 2022GY-380, 2022JQ-533, 2022JQ-139), Natural Science Foundation of Shaanxi Provincial Department of Education (Program No. 22JP100 and No. 22JK0595), Scientific Research Fund for High-Level Talents of Xijing University (No. XJ21B19 and No. XJ21B02), Scientific Research Fund of Xijing University (No. XJ210201) and the Youth Innovation Team of Shaanxi Universities.

Institutional Review Board Statement: Not applicable.

Informed Consent Statement: Not applicable.

Data Availability Statement: The data presented in this study are available on request from the corresponding author.

Conflicts of Interest: The authors declare no conflict of interest.

References

1. Bana, X.; Pang, X.; Li, X.; Hu, B.; Guo, Y.; Zheng, H. A nonlinear plasmonic waveguide based all-optical bidirectional switching. *Opt. Commun.* **2018**, *406*, 124–127. [[CrossRef](#)]
2. Biyiklioglu, Z.; Arslan, T.; Alawainati, F.A.; Manaa, H.; Jaffar, A.; Henari, F.Z. Comparative nonlinear optics and optical limiting properties of metallophthalocyanines. *Inorg. Chim. Acta* **2019**, *486*, 345–351. [[CrossRef](#)]
3. Wen, J.; Ping, L.; Li, R.; Shang, S.; Zhao, W.; Hai, M.; Cao, H.; Yuan, H.; Wang, D.; He, W.; et al. Synthesis and Characterization of New Benzo[e]Indol Salts for Second-Order Nonlinear Optics. *Crystals* **2020**, *10*, 242. [[CrossRef](#)]
4. Liu, J.; Zhang, M.; Gao, W.; Fedorchuk, A.A.; Kityk, I.V. Synthesis and nonlinear optical properties of novel conjugated small molecules based on indole donor. *J. Mol. Struct.* **2018**, *1165*, 223–227. [[CrossRef](#)]
5. Song, Y.D.; Wang, Q.T. Theoretical study of the mixed pi-conjugated bridge effect on the nonlinear optical properties of corannulene derivative. *J. Mol. Model.* **2021**, *27*, 66–76. [[CrossRef](#)]
6. Song, Y.D.; Wang, Q.T. Enhanced nonlinear optical properties of porphyrin with an extended π -conjugated bridge. *Struct. Chem.* **2019**, *30*, 1211–1219. [[CrossRef](#)]
7. Zaier, R.; Mahdhaoui, F.; Ayachi, S.; Boubaker, T. Prediction of structural, vibrational and nonlinear optical properties of small organic conjugated molecules derived from pyridine. *J. Mol. Struct.* **2019**, *1182*, 131–140. [[CrossRef](#)]
8. Li, Y.; Wang, X.; Han, Y.; Sun, H.Y.; Hilborn, J.; Shi, L. Click chemistry-based biopolymeric hydrogels for regenerative medicine. *Biomed. Mater.* **2021**, *16*, 022003. [[CrossRef](#)]
9. Xu, L.; Dong, J. Click Chemistry: Evolving on the Fringe. *Chin. J. Chem.* **2020**, *38*, 414–419. [[CrossRef](#)]
10. Chen, Z.; Liao, C.; Price, R.; Hsu, H.Y.; Younus, M.; Schanze, K.S. Polymeric Nonlinear Absorption Chromophore Array from Controlled Radical Polymerization and “Click” Chemistry. *ACS Appl. Polym. Mater.* **2020**, *2*, 4570–4580. [[CrossRef](#)]
11. Liu, X.; Wang, D.; Gao, H.; Yang, Z.; Xing, Y.; Cao, H.; He, W.; Wang, H.; Gu, J.; Hu, H. Nonlinear optical properties of symmetrical and asymmetrical porphyrin derivatives with click chemistry modification. *Dye. Pigment.* **2016**, *134*, 155–163. [[CrossRef](#)]
12. Zheng, Y.; Zhang, D.; Xu, L.; Hu, Q.; Jing, Z.; Chen, Z.; Wei, D.; Guo, Y.; Jiang, X.F. Bis(phenyltriazolyl)nitroaniline: Click-derived functional materials with highly-transparent and stable two-photon absorption property. *Chem. Phys. Lett.* **2018**, *707*, 80–85. [[CrossRef](#)]
13. Ganesh, M.; Harikrishna, B.; Dana, A.; Anjan, B. Novel series of diaminoanthraquinone-based π -extendable building blocks with tunable optoelectronic properties. *ACS Omega* **2022**, *7*, 25874–25880.
14. He, H.; Wang, C.; Wang, T.; Zhou, N.; Wen, Z.; Wang, S.; He, L. Synthesis, characterization and biological evaluation of fluorescent biphenyl-furocoumarin derivatives. *Dye. Pigment.* **2015**, *113*, 174–180. [[CrossRef](#)]
15. Jires, J.; Gibala, P.; Kalasek, S.; Dousa, M.; Doubisky, J. The determination of two analogues of 4-(azidomethyl)-1,1'-biphenyl as potential genotoxic impurities in the active pharmaceutical ingredient of several sartans containing a tetrazole group. *J. Pharm. Biomed. Anal.* **2021**, *205*, 114300. [[CrossRef](#)] [[PubMed](#)]
16. Liang, X.; Xie, R.; Zhu, C.; Chen, H.; Shen, M.; Li, Q.; Du, B.; Luo, D.; Zeng, L. Comprehensive Identification of Liquid Crystal Monomers-Biphenyls, Cyanobiphenyls, Fluorinated Biphenyls, and their Analogues-in Waste LCD Panels and the First Estimate of their Global Release into the Environment. *Environ. Sci. Technol.* **2021**, *55*, 12424–12436. [[CrossRef](#)]
17. Tan, J.; Cheng, S.M.; Loganath, A.; Chong, Y.S.; Obbard, J.P. Selected organochlorine pesticide and polychlorinated biphenyl residues in house dust in Singapore. *Chemosphere* **2007**, *68*, 1675–1682. [[CrossRef](#)]
18. Kim, S.; Park, C.; Lee, J. Reduction of polycyclic compounds and biphenyls generated by pyrolysis of industrial plastic waste by using supported metal catalysts: A case study of polyethylene terephthalate treatment. *J. Hazard. Mater.* **2020**, *392*, 122464. [[CrossRef](#)]
19. Lee, W.H.; Kim, Y.S.; Bae, C. Robust Hydroxide Ion Conducting Poly(biphenyl alkylene)s for Alkaline Fuel Cell Membranes. *ACS Macro Lett.* **2015**, *4*, 814–818. [[CrossRef](#)]
20. Zhang, S.; Wang, Y.; Liu, P.; Wang, X.; Zhu, X. Photo-cross-linked poly(N-allylisatin biphenyl)-co-poly(alkylene biphenyl)s with pendant N-cyclic quaternary ammonium as anion exchange membranes for direct borohydride/hydrogen peroxide fuel cells. *React. Funct. Polym.* **2020**, *152*, 104576. [[CrossRef](#)]
21. Wang, T.F.; Huang, W.B.; Sun, T.; Zhang, W.X.; Tang, W.; Yan, L.H.; Si, J.H.; Ma, H.P. Two-dimensional metal-polyphthalocyanine conjugated porous frameworks as promising optical limiting materials. *ACS Appl. Mater. Inter.* **2020**, *12*, 46565–46570. [[CrossRef](#)] [[PubMed](#)]
22. Liu, G.C.; Liao, Q.Y.; Deng, H.Y.; Zhao, W.I.; Chen, P.Y.; Tang, R.L.; Li, Q.Q.; Li, Z. Janus NLO dendrimers with different peripheral functional groups: Convenient synthesis and enhanced NLO performance with the aid of the Ar-ArF self-assembly. *J. Mater. Chem. C* **2019**, *7*, 7344–7351. [[CrossRef](#)]
23. Liu, J.L.; Huo, F.Y.; He, W.Q. Construction of a simple crosslinking system and its influence on the poling efficiency and orientational stability of organic electro-optic materials. *RSC Adv.* **2020**, *10*, 6482–6490. [[CrossRef](#)] [[PubMed](#)]

24. Liu, X.; Wang, D.; Gao, H.; Yang, Z.; Xing, Y.; Cao, H.; He, W.; Wang, H.; Gu, J.; Hu, H. Click chemistry functionalization improving the wideband optical-limiting performance of fullerene derivatives. *Phys. Chem. Chem. Phys.* **2016**, *18*, 7341–7348. [[CrossRef](#)]
25. Mi, Y.S.; Liang, P.X.; Jin, Z.K.; Wang, D.; Yang, Z. Synthesis and third-order nonlinear optical properties of triphenylene derivatives modified by click chemistry. *Phys. Chem. Chem. Phys.* **2013**, *14*, 4102–4108. [[CrossRef](#)]
26. Michinobu, T.; May, J.C.; Lim, J.H.; Boudon, C.; Gisselbrecht, J.P.; Seiler, P.; Gross, M.; Biaggio, I.; Diederich, F. A new class of organic donor-acceptor molecules with large third-order optical nonlinearities. *Chem. Commun.* **2005**, *6*, 737–739. [[CrossRef](#)]
27. Miao, Z.C.; Han, H.H.; Wang, D.; Gao, H.; Gu, J.M.; Hu, H.Y. Nonlinear optical and energy-level modulation of organic alkynes by click chemistry. *Tetrahedron* **2016**, *72*, 4039–4046. [[CrossRef](#)]
28. Varotto, A.; Nam, C.Y.; Radivojevic, I.; Tom, J.P.C.; Cavaleiro, J.A.S.; Black, C.T.; Drain, C.M. Phthalocyanine blends improve bulk heterojunction solar cells. *J. Am. Chem. Soc.* **2010**, *132*, 2552–2554. [[CrossRef](#)]
29. Kim, J.; Lee, J.; Chae, S.; Shim, J.Y.; Lee, D.Y.; Kim, I.; Kim, H.J.; Park, S.H.; Suh, H. Conjugated polymers containing pyrimidine with electron withdrawing substituents for organic photovoltaics with high open-circuit voltage. *Polymer* **2016**, *83*, 50–58. [[CrossRef](#)]
30. Hatano, T.; Stopa, M.; Tarucha, S. Single-electron delocalization in hybrid vertical-lateral double quantum dots. *Science* **2005**, *309*, 268–271. [[CrossRef](#)]
31. Yoshioka, K.; Minami, Y.; Shudo, K.; Dao, T.D.; Nagao, T.; Kitajima, M.; Takeda, J.; Katayama, I. Terahertz-field-induced nonlinear electron delocalization in Au nanostructures. *Nano Lett.* **2015**, *15*, 1036–1040. [[CrossRef](#)] [[PubMed](#)]
32. Li, Y.R.; Tsuboi, K.; Michinobu, T. Double click synthesis and second-order nonlinearities of polystyrenes bearing donor-acceptor chromophores. *Macromolecules* **2010**, *43*, 5277–5286. [[CrossRef](#)]
33. Yildirim, M.; Kaya, I. Soluble semi-conductive chelate polymers containing Cr (II) in the backbone: Synthesis, characterization, optical, electrochemical, and electrical properties. *Polymer* **2009**, *50*, 5653–5660. [[CrossRef](#)]
34. Han, P.B.; Yang, Z.; Cao, H.; He, W.L.; Wang, D.; Zhang, J.J.; Xing, Y.; Gao, H. Nonlinear optical properties of the novel kind of organic donor-acceptor thiophene derivatives with click chemistry modification. *Tetrahedron* **2017**, *73*, 6210–6216. [[CrossRef](#)]
35. Jin, Z.K.; Wang, D.; Wang, X.K.; Liang, P.X.; Mi, Y.S.; Yang, H. Efficient modification of pyrene-derivative featuring third-order nonlinear optics via the click post-functionalization. *Tetrahedron Lett.* **2013**, *54*, 4859–4864. [[CrossRef](#)]